

UPCommons

Portal del coneixement obert de la UPC

<http://upcommons.upc.edu/e-prints>

© 2019 IEEE. Personal use of this material is permitted. Permission from IEEE must be obtained for all other uses, in any current or future media, including reprinting/republishing this material for advertising or promotional purposes, creating new collective works, for resale or redistribution to servers or lists, or reuse of any copyrighted component of this work in other Works.

Aquesta és una còpia de la versió author's final draft del treball a Study of modulation techniques applied to full bridge single-phase inverters based on wide-bandgap semiconductors publicat a "IECON 2019: 45th Annual Conference of the IEEE Industrial Electronics Society: Convention Center, Lisbon, Portugal: 14-17 October, 2019"

URL d'aquest document a UPCommons E-prints:
<http://hdl.handle.net/2117/175800>

Article publicat / *Published paper:*

Ferrer-Arnau, L. [et al.]. Study of modulation techniques applied to full bridge single-phase inverters based on wide-bandgap semiconductors. A: Annual Conference of the IEEE Industrial Electronics Society. "IECON 2019: 45th Annual Conference of the IEEE Industrial Electronics Society: Convention Center, Lisbon, Portugal: 14-17 October, 2019". 2019, p. 2032-2037.

Study of modulation techniques applied to full bridge single-phase inverters based on wide-bandgap semiconductors

Lluís Ferrer-Arnau

Department of Electronic Engineering
Universitat Politècnica de Catalunya
Terrassa, Spain

luís.jorge.ferrer@upc.edu

Nestor Berbel

Department of Electronic Engineering
Universitat Politècnica de Catalunya
Terrassa, Spain

nestor.berbel-artal@upc.edu

Gabriel J. Capella

Department of Electronic Engineering
Universitat Politècnica de Catalunya
Terrassa, Spain

gabriel.jose.capella@upc.edu

Jordi Zaragoza

Department of Electronic Engineering
Universitat Politècnica de Catalunya
Terrassa, Spain

jordi.zaragoza-bertomeu@upc.edu

Abstract—Wide-band gap (WBG) devices are gradually replacing standard Si/SiC semiconductors in power converters. This is due to the fact that WBG devices exhibit lower capacitance and on-resistance and besides, as they can switch at much higher frequencies, high-quality output voltage can be achieved. Additional improvements can be obtained by using new modulation techniques. In this paper, four modulation techniques (Bipolar, Unipolar, Discontinuous 1P and Discontinuous 2P) have been studied. All of them have been implemented on a WBG based full-bridge single-phase inverter. In order to assess the output voltage quality, Total Harmonic Distortion (THD) and Weighted Total Harmonic Distortion (WTHD) have been computed. Overall power losses and Common Mode Voltage (CMV) have been computed too. In terms of output quality, better results are obtained with either unipolar or any of the discontinuous modulation techniques. Discontinuous techniques show also excellent results as for power losses. The best CMV results are obtained with bipolar modulation.

Keywords—GaN, modulation techniques, power quality, efficiency, power inverter.

I. INTRODUCTION

The latest wide bandgap (WBG) devices, such as Gallium Nitride (GaN) transistors, are nowadays preferred to conventional silicon power devices [1]. GaN devices qualify for their use at high switching frequencies, because of the higher saturation velocity and lower input and output capacitances, and high-efficiency. Due to their lower on-resistance when compared to Si transistors, they exhibit a higher efficiency [2][3]. However, GaN devices have some drawbacks, such as a higher forward voltage drop in the GaN Schottky Diode, in comparison to Si Schottky Diodes [4].

In power converters, such as single-phase and three-phase inverters, traditional power devices can be replaced by wide bandgap (WBG) devices, so that the switching frequency can be increased, the heat sink size reduced, and the output filter can be reduced as well [5]. Due to the use of WBG devices, the harmonic distortion and the efficiency of the power converter can be improved, but it can also be boosted by the use of new modulation techniques. The most common modulation techniques used in half-bridge and full-bridge inverters are unipolar and bipolar sinusoidal pulse width modulation (PWM) techniques, in which a sinusoidal signal is compared with a triangular signal in order to produce the gate control signal for the power devices [6]. The common mode voltage can inject harmonic components in the high-frequency

range, which produce electromagnetic interference (EMI) problems [7], therefore, the appropriate modulation technique should be chosen according to the application.

This paper studies the switching and conduction losses, the output power quality and the CMV generated in a single-phase inverter made up with GaN power devices. To that extent, a comparison of different modulation techniques that include unipolar, bipolar and two different discontinuous-modulation techniques is performed.

The rest of the paper is organized as follows: in Section II the methods to calculate the losses in the power devices, the output voltage quality parameters and the common mode voltage are explained. The modulation techniques are summarized in Section III. The simulation model and the comparison of the results are described in Section IV. Experimental results are presented in Section V. The paper conclusions are drawn in Section VI.

II. SEMICONDUCTOR LOSSES, OUTPUT VOLTAGE QUALITY AND COMMON MODE VOLTAGE

The parameters which will be used to assess the performance of the different modulation techniques, i. e. the semiconductor losses, the output voltage quality and the common mode voltage, are presented in this Section. All these schemes are implemented on a single-phase full-bridge inverter (Fig. 1).

A. Semiconductor losses.

In power electronic devices, power losses can be classified into conduction and switching losses [8][9][10]. Conduction losses are due to the voltage drop across the device when the FET transistors are in their ohmic zone. Conduction losses can be approximated by means of (1).

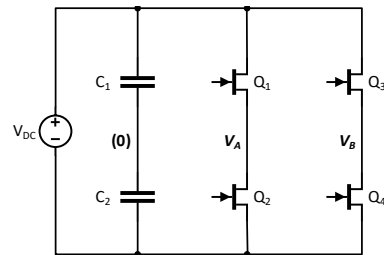


Fig. 1. Full-bridge Inverter.

$$P_{cl} = \frac{1}{T_{sw}} \cdot \int_0^{T_{sw}} V_{FO} \cdot i_D \cdot dt. \quad (1)$$

Where V_{FO} is the device threshold voltage, i_D is the device current, and T_{sw} is the switching period.

Switching losses occur when the FET transistor switches from its ohmic zone to the cut-off zone and vice-versa. Due to the lack of reverse recovery charge, the switching losses on GaN devices are less than those of Si and SiC transistors [11]. Switching losses are difficult to measure [12][13][14], but they can be approximated by

$$P_{sl} = \frac{1}{n \cdot T_{sw}} \cdot \sum_{i=1}^{n \cdot T_{sw}} \left[E_{on}(v_{block}, i_D, T_j) \Big|_i + E_{off}(v_{block}, i_D, T_j) \Big|_i \right]. \quad (2)$$

Where $n \cdot T_{sw}$ is the number of transitions in one fundamental period and E_{on} and E_{off} are the energy dissipated during the turn-on and turn-off transitions, respectively. Such energies depend on the FET blocking voltage, v_{block} , the device current, i_D , and the junction temperature, T_j .

B. Output voltage quality.

The quality of the output voltage waveforms is evaluated by using two parameters: total harmonic distortion (THD) and weighted total harmonic distortion (WTHD), also called distortion factor. Unlike THD, WTHD takes into account the frequency of the harmonics so that the low-frequency harmonics weigh more than the high-frequency ones. The parameters are defined by means of (3) and (4) [15].

$$THD(\%) = 100 \cdot \sqrt{\frac{\sum_{n=2}^{\infty} V_{n,rms}^2}{V_{1,rms}^2}} = 100 \cdot \sqrt{\left(\frac{V_{rms}}{V_{1,rms}}\right)^2 - 1}, \quad (3)$$

$$WTHD(\%) = 100 \cdot \sqrt{\frac{\sum_{n=2}^{\infty} \left(\frac{V_{n,rms}}{n}\right)^2}{V_{1,rms}^2}}. \quad (4)$$

C. Common Mode Voltage

CMV in photovoltaic (PV) applications can cause ground leakage current which might originate problems of EMI, personnel safety, power quality issues and system losses. In order to evaluate the CMV amplitudes that occur under specific operating conditions of the converter, the normalized parameter (E_{norm}) has been used (5).

$$E_{norm} \approx \sum_{n=1}^{\infty} \left[\frac{V_n}{V_{DC}} \right]^2 \quad (5)$$

Where V_n is the amplitude of the n harmonic of the CMV signal (7), and V_{DC} is dc bus voltage.

III. MODULATION TECHNIQUES

Fig. 2 shows the modulation signals used for the different modulation techniques. Bipolar and unipolar modulations are sheer sinusoidal PWM techniques, whereas in the discontinuous modulation techniques 1P and 2P, the modulation signals are not continuous and have been modified in order to improve the power converter performance by reducing the switching losses.

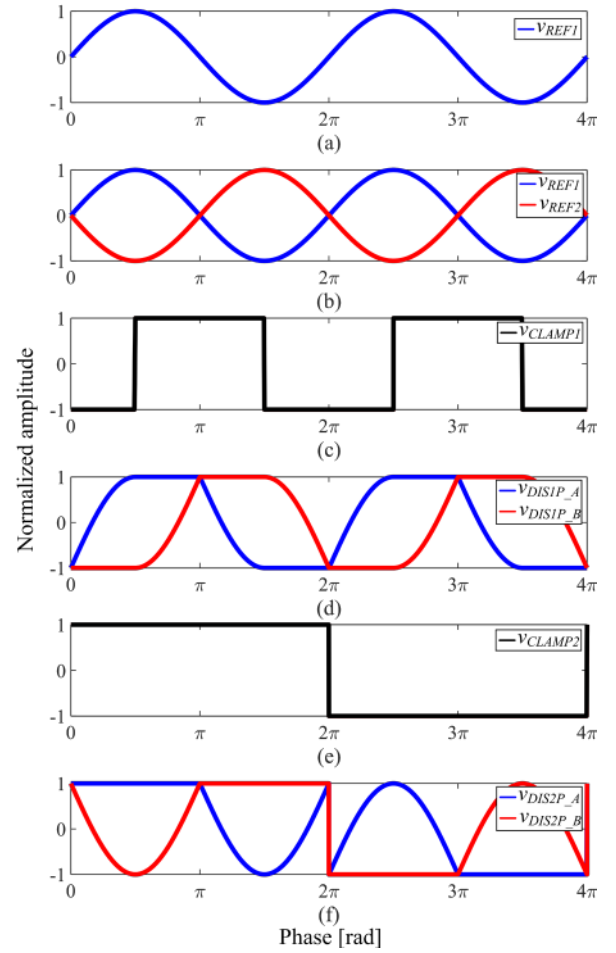


Fig. 2. Modulation signal waveforms for $m=1$: (a) Bipolar, (b) Unipolar, (c) Clamping signal for Discontinuous 1P, (d) Discontinuous 1P, (e) Clamping signal for Discontinuous 2P, and (f) Discontinuous 2P.

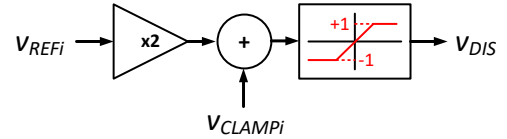


Fig. 3. Line-to-line voltage spectra with bipolar modulating signal.

The control signals of the GaN devices in all the PWM techniques are generated by comparison of a carrier signal with one or two modulation signals. In bipolar modulation a single modulation signal is used, whereas in unipolar and discontinuous modulations, a different modulation signal is used for each leg of the converter [16]. In unipolar modulation, the two modulation signals are π radians phase-shifted sinusoidal signals, namely V_{REF1} and V_{REF2} .

In order to generate the modulation signals for both legs of the inverter when using discontinuous modulations, the aforementioned sinusoidal reference signals are modified as follows: a clamping signal (V_{clamp1} or V_{clamp2}) is added to twice the reference signals and the result is truncated to either +1 or -1 (Fig. 3).

The period of the clamping signal for discontinuous modulation 1P (V_{CLAMP1}) is the same as for the reference signal, V_{REF1} . The period of the clamping signal for discontinuous modulation 2P (V_{CLAMP2}) is twice the period of the reference signal. The clamping signals and the modulation

signals for both discontinuous modulation 1P and 2P can be seen in Fig. 2(c) and Fig. 2(e), respectively.

In discontinuous 1P, the clamping signal, V_{CLAMP1} , switches between +1 and -1 everytime the reference signals reaches a peak value: i.e. at $(2n+1) \cdot \pi/2$, for $n = \{0, 1, 2, \dots\}$. In discontinuous 2P, the clamping signal, V_{CLAMP2} , switches between +1 and -1 everytime the reference signals begin a new full period, i.e. at $2 \cdot n \cdot \pi$, for $n = \{0, 1, 2, \dots\}$

By means of the discontinuous switching techniques, while one of the legs of the full-bridge converter is switching at f_{sw} frequency, the other leg remains clamped at either 0 V or V_{DC} , thus reducing the overall switching losses.

IV. SIMULATION MODEL AND RESULTS

All the modulation techniques and the full bridge single-phase converter are implemented in Matlab/Simulink and PLECS blockset software. This software allows the engineer to study the thermal losses of the system. Conduction and switching losses are calculated by means of look-up tables, which take into account the device junction temperature and the device current and voltage.

The GaN power device model GS66516B has been used in this analysis. Table 1 shows the simulation parameters of the system.

TABLE I. SIMULATION PARAMETERS

Switching frequency (f_{sw})	10kHz, 50kHz, 100kHz and 200kHz
Voltage Source (V_{DC})	400 V
Load current (rms)	30 A
Junction Temperature (T)	25°C

In this study, four types of simulations have been carried out. The first simulations are detailed in Section IV-A, and the different output spectra of the line-to-line voltage are compared. The second simulations, which are explained in Section IV-B, demonstrate the switching and conduction losses for the four types of modulation techniques and for four different switching frequencies. In Section IV-C THD and WTHD for all the modulation techniques are compared. Finally, in Section IV-D, the CMV for the different modulation techniques are analyzed.

A. Line-to-line output voltage spectra comparison.

Figs. 4, 5, 6 and 7 plot the output spectra of the line-to-line voltage for the four modulating techniques. The simulation has been performed for two different switching frequencies, 10 kHz and 100 kHz, and for a modulating index (m_a) of 0.5. The line-to-line voltage is presented in a normalized amplitude, as detailed in (6)

$$V_{ab}(f) = FT \left\{ \frac{V_{ab}(t)}{V_{DC}} \right\}. \quad (6)$$

Due to the increase of the switching frequency, the harmonic content is shifted towards higher frequencies, so that the size of the output filter can be reduced. Bipolar modulation technique presents harmonic content with the highest amplitudes (Fig. 4), and discontinuous 2P technique renders the lowest harmonic content (Fig. 7). Furthermore, it can be observed that with the unipolar modulation the first unwanted

harmonic appears at a frequency that is twice the switching frequency. In order to evaluate the harmonic content, THD and WTHD are computed.

B. THD and WTHD.

In Section IV-A, the harmonic content of the line-to-line voltage has been plotted. In order to assess which modulation technique show the best results, THD and WTHD have been computed and the results can be seen in Section IV-B. Fig. 8 depicts the THD for different modulation indexes at a switching frequency of 50 kHz, although THD is not affected by the switching frequency. Unipolar, discontinuous 1P and discontinuous 2P modulations yield a better THD when compared to the bipolar modulation technique, because the line-to-line has three voltage levels (V_{DC} , 0 V and $-V_{DC}$) whereas, with the bipolar modulating technique, the line-to-line voltage has only two voltage levels: V_{DC} and $-V_{DC}$. A zoomed plot of the THD for modulation indexes ranging from 0.7 to 1 has been included in Fig. 8. It can be observed that unipolar, discontinuous 1P and discontinuous 2P techniques improve the THD with regards to the bipolar one by more than 50 %.

Figs. 9, 10 and 11 illustrate the WTHD for different modulation indexes, for switching frequencies of 10 kHz, 50 kHz, 100 kHz and 200 kHz. In all modulation techniques can be observed that, as the switching frequency increases, the WTHD is reduced because of the fact that the harmonic content is shifted to the high-frequency area, as depicted in Figs. 4 to 7. The unipolar and discontinuous 1P and 2P modulation techniques present a lower WTHD in comparison to the bipolar modulation technique.

C. Conduction and switching losses comparison.

With the help of PLECS software and taking into account the GaN transistor characteristic curves, several simulations have been run in order to estimate the conduction and switching losses for the four modulating techniques. Conduction and switching losses have been calculated for a modulation index of 1 and for an output current in phase with the line-to-line voltage. The results are plotted in Fig. 12. Conduction and switching losses are very similar in bipolar and unipolar modulation techniques, and for the discontinuous 1P and 2P, regardless of the switching frequency. Basically, the number of commutations in one period of the modulating signal is the same in the cases of bipolar and the unipolar, and the same for discontinuous 1P and 2P.

The discontinuous modulation techniques, either 1P or 2P, produce lower losses than the bipolar or unipolar modulation techniques. At low switching frequencies, the total losses are almost the same, but as the switching frequency increases, the discontinuous 1P and 2P modulation techniques are better than the two others. At a switching frequency of 200 kHz, the total losses amount up to 83.7 W for the discontinuous 1P and 2P, whereas the bipolar and unipolar techniques total losses are 118.17 W.

The discontinuous modulation techniques are better, in terms of switching losses, because of the fact that for certain intervals (Fig. 2), the modulating signal is clamped at 1 or -1, so the overall number of commutations is reduced.

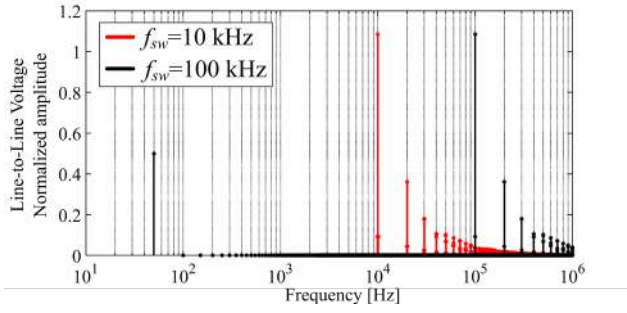


Fig. 4. Line-to-line voltage spectra with bipolar modulating signal.

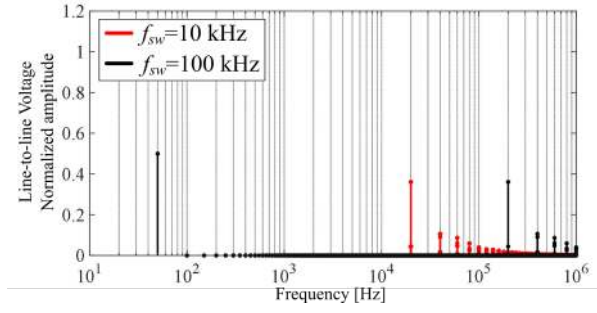


Fig. 5. Line-to-line voltage spectra with unipolar modulating signal.

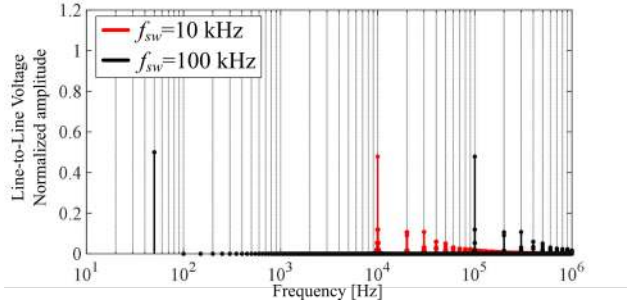


Fig. 6. Line-to-line voltage spectra with discontinuous 1P modulating signal.

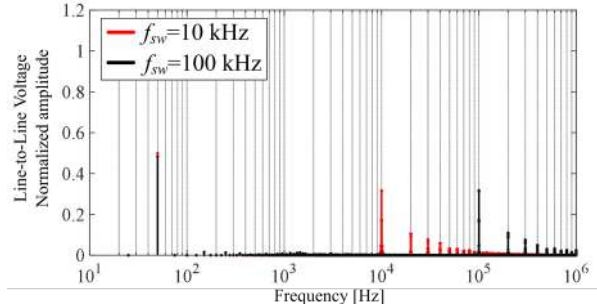


Fig. 7. Line-to-line voltage spectra with discontinuous 2P modulating signal.

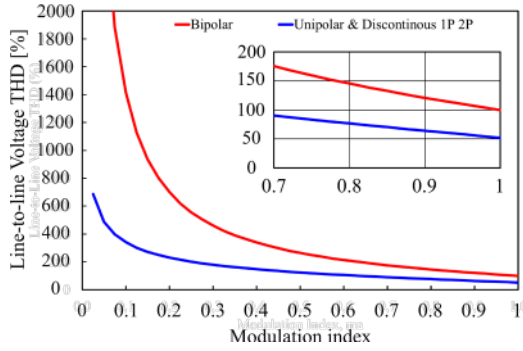


Fig. 8. THD for all modulating signals at 50 kHz switching frequency.

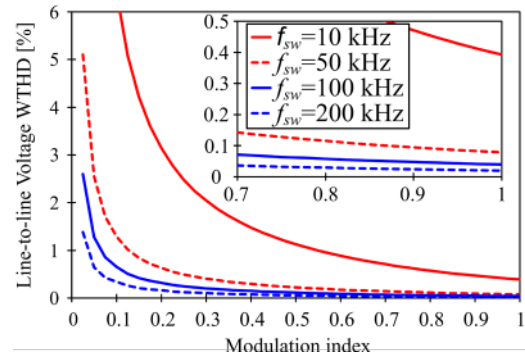


Fig. 9. WTHD for the bipolar modulating signal.

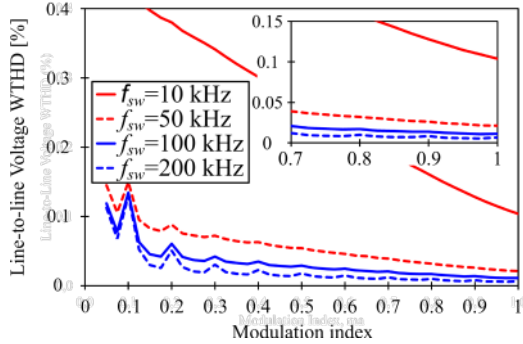


Fig. 10. WTHD for the unipolar modulating signal.

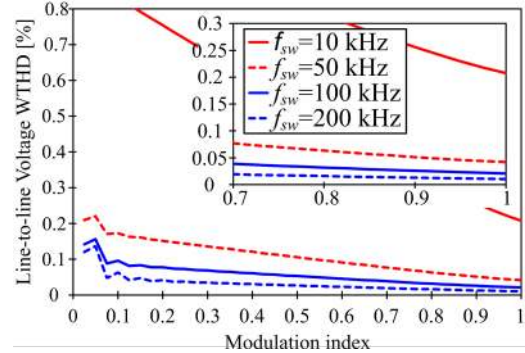


Fig. 11. WTHD for the discontinuous 1P and 2P modulating signal.

D. Common Mode Voltage.

The common mode voltage is computed by means of (7).

$$V_{CM} = \frac{V_{AO} + V_{BO}}{2} \quad (7)$$

Where V_{AO} and V_{BO} are the mid-point voltages of each leg of the full-bridge (Fig.1). The CMV is obtained for several

switching frequencies and for a modulation index of 1. The energy of the CMV (5) for the four modulation techniques is plotted in Fig. 14. Bipolar modulation technique does not generate any CMV because V_{AO} and V_{BO} are complementary and they switch synchronously. Furthermore, in terms of CMV the unipolar and both discontinuous modulation techniques present the same result. The CMV spectrum is shown in Figs. 15 to 17 for the unipolar, discontinuous 1P and 2P modulation techniques, respectively. It can be seen that

the unipolar modulation (Fig. 15) does not show low frequency components in its spectrum. On the contrary, the discontinuous 1P and 2P (Figs. 16 and 17) really do show low frequency components in their spectra, i.e. harmonics at the grid fundamental frequency and at its multiples and submultiples. The appearance of this components are due, once again, to the modulating signals being clamped at +1 or -1 for certain intervals.

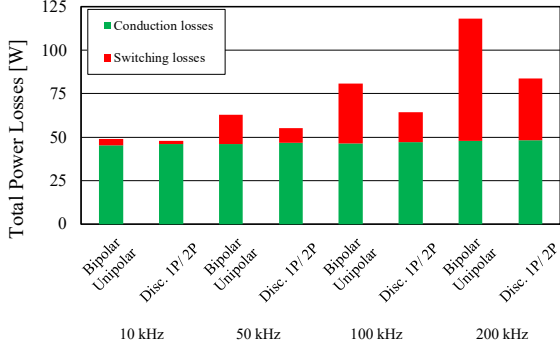


Fig. 12. Total losses at different switching frequencies for the bipolar, unipolar, discontinuous 1P and 2P modulation techniques.

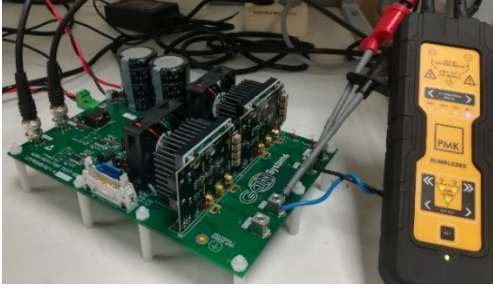


Fig. 13. Experimental platform.

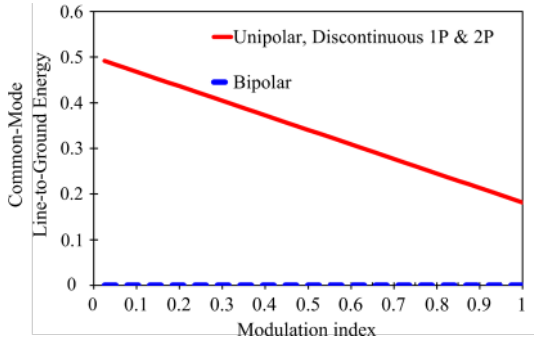


Fig. 14. Energy of the Common-mode voltage.

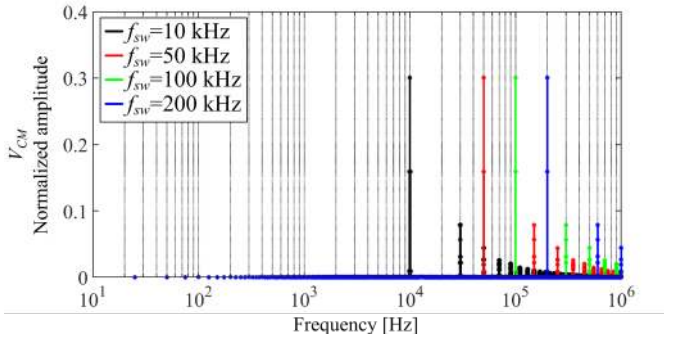


Fig. 15. CMV Spectrum for the unipolar modulation technique.

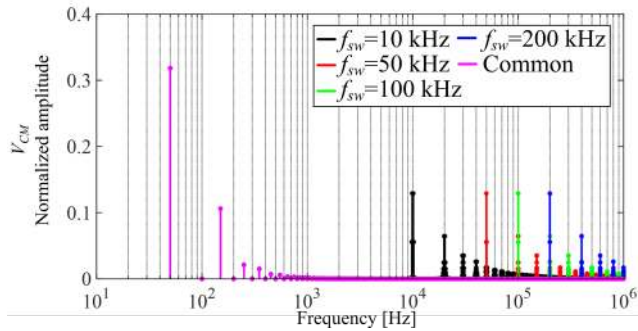


Fig. 16. CMV Spectrum for the discontinuous 1P modulation technique.

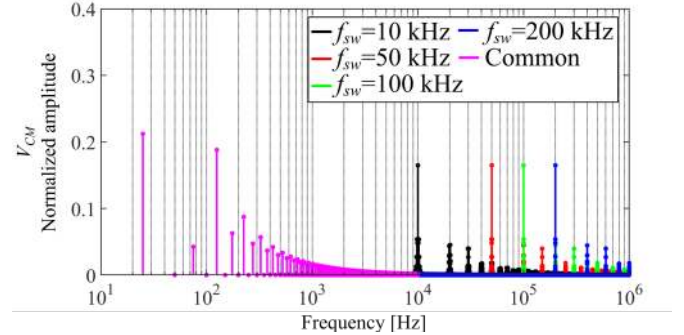


Fig. 17. CMV Spectrum for the Discontinuous 2P modulation technique.

V. EXPERIMENTAL RESULTS

Experimental results have been obtained with the GSP65MB evaluation board of GaN systems with a RL load (Fig. 13). The modulation techniques have been implemented with the dSpace DS1006. The line-to-line voltage has been measured with the BumbleBee Differential HV-Probe, which has a 400 MHz bandwidth. Parameters of the experimental setup are summarized in Table II. THD and WTHD of the experimental line-to-line voltage results have been calculated. THD results for switching frequencies of 10 kHz and 100 kHz can be seen in Tables III and IV. As simulation results anticipated, a reduction on THD is achieved as the modulations index increases. Experimental WTHD results are shown in Tables V and VI, and they perfectly match simulation results.

TABLE II. EXPERIMENTAL SETUP PARAMETERS

FET	GS66516B
V_{DC}	400 V
Switching frequency	10 kHz / 100 kHz
R	68 Ω
L	45 μ H

VI. CONCLUSIONS

A comparison of four modulation techniques (bipolar, unipolar and two discontinuous modulation techniques) applied to a GaN full-bridge single-phase inverter is presented in this paper. Switching and conduction losses, as well as CMV and output voltage quality have been considered at different switching frequencies. Simulation results have been experimentally corroborated.

TABLE III. THD 10 kHz SWITCHING FREQUENCY

m	Unipolar	Bipolar	Dis-1P	Dis-2P
	$f_{sw}=10$ kHz			
0.7	90.41 %	174.29 %	90.18 %	90.15 %
0.8	77.47 %	144.88 %	76.75 %	76.73 %
0.9	64.58 %	120.55 %	64.29 %	64.30 %

TABLE IV. THD 100 kHz SWITCHING FREQUENCY

m	Unipolar	Bipolar	Dis-1P	Dis-2P
	$f_{sw}=100$ kHz			
0.7	97.11 %	181.48 %	94.69 %	94.73 %
0.8	82.95 %	151.27 %	80.87 %	80.87 %
0.9	80.87 %	126.13 %	68.10 %	68.11 %

TABLE V. WTHD 10 kHz SWITCHING FREQUENCY

m	Bipolar	Unipolar	Dis-1P	Dis-2P
	$f_{sw}=10$ kHz			
0.7	0.70 %	0.19 %	0.47 %	0.41 %
0.8	0.57 %	0.16 %	0.31 %	0.33 %
0.9	0.47 %	0.13 %	0.27 %	0.26 %

TABLE VI. WTHD 100 kHz SWITCHING FREQUENCY

m	Bipolar	Unipolar	Dis-1P	Dis-2P
	$f_{sw}=100$ kHz			
0.7	0.088 %	0.060 %	0.076 %	0.077 %
0.8	0.080 %	0.058 %	0.068 %	0.069 %
0.9	0.064 %	0.068 %	0.051 %	0.062 %

Switching and conduction losses, as well as CMV and output voltage quality have been considered at different switching frequencies. Simulation results have been experimentally corroborated.

The results of the study show that every modulation technique beats the others in some specific aspects. To that extend, bipolar modulation technique delivers output voltage with no CMV, however the THD and WTHD values are the highest of all four techniques. Unipolar modulation technique provides better output voltage quality despite not generating a CMV-free output voltage. Neither of discontinuous modulation techniques guaranty an output voltage free of CMV component. However, they are the best ones in terms of power losses, which implies a better efficiency of the converter.

It can be concluded that, depending on the the type of converter application, the optimal modulation technique should be selected. For example, in photovoltaic applications, where the absence of CMV is crucial in order not to damage the pannels, bipolar modulation is the appropriate one. In grid connected inverters, in order to minimize the size of the filter required and to maximize converter efficiency, modulation strategies like discontinuous 1P and 2P are the most appropriate.

High-frequency switching can be used in power converters implemented with WBG devices. As a consequence, reactive

components can be smaller. Among the four modulation techniques studied, discontinuous modulations, either DIP or D2P, are the ones that exhibit low switching losses and present a significant reduction when compared with either unipolar or bipolar techniques.

ACKNOWLEDGMENT

This work was supported by the “Secretaria d’Universitats i Recerca del Departament d’Empresa i Coneixement de la Generalitat de Catalunya”.

REFERENCES

- [1] E. A. Jones, F. F. Wang, and D. Costinett, “Review of Commercial GaN Power Devices and GaN-Based Converter Design Challenges,” *IEEE J. Emerg. Sel. Top. Power Electron.*, vol. 4, no. 3, pp. 707–719, Sep. 2016.
- [2] K. Cen, Z. Jianjun, K. Yuechan, Z. Kai, and C. Tangsheng, “Enhancement-mode GaN HEMT power electronic device with low specific on resistance,” in *Proc. China International Forum on Solid State Lighting: International Forum on Wide Bandgap Semiconductors China (SSLChina: IFWS)*, 2017, pp. 183–185.
- [3] J. Millan, P. Godignon, X. Perpina, A. Perez-Tomas, and J. Rebollo, “A Survey of Wide Bandgap Power Semiconductor Devices,” *IEEE Trans. Power Electron.*, vol. 29, no. 5, pp. 2155–2163, May 2014.
- [4] B. Ozpineci and L. M. Tolbert, “Comparison of Wide-Bandgap Semiconductors for Power Electronics Applications,” 2003.
- [5] E. Gurpinar and A. Castellazzi, “Single-Phase T-Type Inverter Performance Benchmark Using Si IGBTs, SiC MOSFETs and GaN HEMTs,” *IEEE Trans. Power Electron.*, vol. 31, no. 10, pp. 7148 - 7160, Oct. 2016.
- [6] P. Roy, J. N. Bera, G. Sarkar, and S. Chowdhuri, “A Study on Filter Design Aspects of Single-Phase Inverter with Various Modulation Schemes,” Springer, Singapore, 2019, pp. 17–24.
- [7] P. Pairodamonchai, “Impact of PWM Modulation Schemes on Common-Mode Voltage Generated by 3-Level Neutral-Point-Clamped Inverters,” in *Proc. Conf. on Engineering Science and Innovative Technology (ESIT)*, 2018, pp. 1–5.
- [8] J. Pou, D. Osorno, J. Zaragoza, C. Jaen, and S. Ceballos, “Power losses calculation methodology to evaluate inverter efficiency in electrical vehicles,” in 2011 7th International Conference-Workshop Compatibility and Power Electronics (CPE), 2011, pp. 404–409.
- [9] K. Rouzbehi *et al.*, “Comparative efficiency study of single phase photovoltaic grid connected inverters using PLECS®,” in *Proc. International Congress on Technology, Communication and Knowledge (ICTCK)*, 2015, pp. 536–541.
- [10] A. Wintrich, U. Nicolai, W. Tursky, and T. Reimann, “Application Manual Power Semiconductors,” 2015.
- [11] X. Ding, Y. Zhou, and J. Cheng, “A Review of Gallium Nitride Power Device and Its Applications in Motor Drive,” *China Electrotech. Soc. Trans. Electr. Mach. Syst.*, vol. 3, no. 1, pp. 54–64, Apr. 2019.
- [12] J. Xu, Y. Qiu, D. Chen, J. Lu, R. Hou, and P. Di Maso, “An Experimental Comparison of GaN E-HEMTs versus SiC MOSFETs over Different Operating Temperatures,” in *Bodo's Power System*, June, 2017.
- [13] R. Hou, J. Lu, and D. Chen, “Parasitic capacitance Eloss loss mechanism, calculation, and measurement in hard-switching for GaN HEMTs,” in *Proc. IEEE Applied Power Electronics Conference and Exposition (APEC)*, 2018, pp. 919–924.
- [14] GaN Systems, “GN003 Application Note Measurement Techniques for High-Speed GaNE-HEMTs,” 2018.
- [15] D. G. Holmes and T. A. Lipo, *Pulse width modulation for power converters : principles and practice*. John Wiley, 2003.
- [16] J. Soomro, T. D. Memon, and M. A. Shah, “Design and analysis of single phase voltage source inverter using Unipolar and Bipolar pulse width modulation techniques,” in *Proc. International Conference on Advances in Electrical, Electronic and Systems Engineering (ICAEES)*, 2016, pp. 277–282.